The Use of Abaqus in an Engine Bearing Design Environment

David R Merritt, Omar Mian

Mahle Engine Systems Ltd., UK

Abstract:

Mahle Engine Systems has developed and maintains an internal software code called SABRE-EHL for Elastohydrodynamic (EHD) bearing simulation. The target components are oil lubricated journal bearings within an internal combustion engine, primarily the crankshaft bearings, small end bushes, camshaft and balancer shaft bearings. The SABRE-EHL tool is used to optimize bearing design and investigate customer problems.

Abaqus is an integral part of the analysis process, proving data related to the structural stiffness of the housing, assembly deformations, inertia effects and journal/crankpin misalignment. This paper provides an overview of the different types of Abaqus analysis which have been developed and deployed in order to extract the required input data for SABRE-EHL.

In addition to providing input data to SABRE-EHL, Abaqus can also be used to apply bearing pressures back onto the structural model. SABRE-EHL oil film pressures are mapped onto the Abaqus bearing mesh and used to perform a non-linear engine cycle analysis where housing stresses and detailed housing-bearing contact interactions can be investigated.

Keywords: Automotive, Journal Bearings, Assembly Deformation, Bolt Loading, Elasticity, Experimental Verification, Powertrain, Substructures, Elastohydrodynamic, Lubrication

1. Introduction

The internal combustion engine relies on fluid-film plain journal bearings as an essential component present within the cranktrain. Their main purpose is the generation of a hydrodynamic oil film between the bearing surface and rotating journal which is at sufficient pressure to transmit and support the firing and inertia loads without excessive asperity contact and friction (Figure 1). They also perform a vital role in temperature control, conducting heat through the bearing into the housing and also convecting heat away in oil flowing out of the bearing sides.

In order to perform this role satisfactorily a bearing material requires a number of key properties:

- Strength, to survive millions of cycles at high load without fatigue damage.
- Wear resistance, to prevent excessive wear which could lead to increased clearance and possibly removal of the bearing overlay material within the lifetime of the engine.
- Conformability, enabling the bearing to accommodate geometry misalignments with the journal via localized beneficial wear and polishing of the surface asperities.

- Compatibility (seizure resistance), allowing asperity contact 'scuff' events without 'friction welding' of the bearing material with the journal.
- Embedability, enabling the material to entrap foreign particle debris circulating in the oil which otherwise could cause excessive scratches and scuff events leading to seizure.

The properties required for strength and wear resistance are in opposition to the properties required for conformability, compatibility and embedability and need to be held in balance. To meet these requirements bearings are generally constructed in a composite bi-layer or tri-layer structure, with a harder material used for the base layer (steel), less hard materials used for the bearing lining (aluminium or copper alloy) and in the case of tri-layer bearings a final thin overlay of softer material.

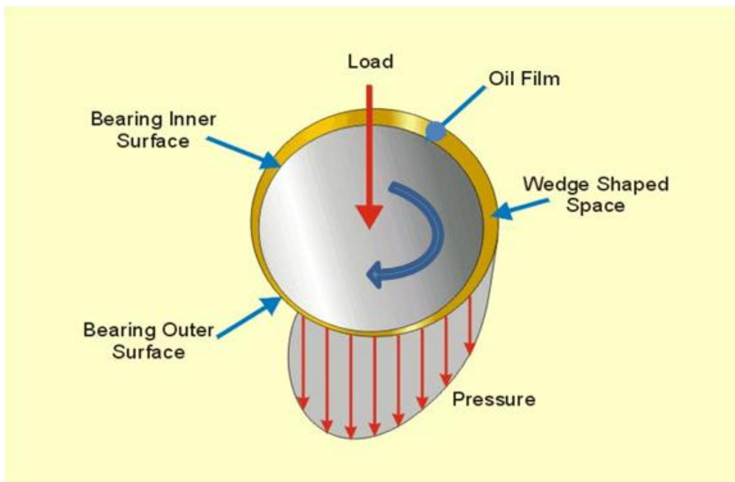

Figure 1: Hydrodynamic pressure generation in a plain journal bearing.

There is on-going pressure in the automotive industry to increase performance, improve efficiency and reduce emissions (CO_2). Design strategies to achieve these goals include: turbo-charging, engine downsizing, increased cylinder pressure, lower viscosity oils, component mass reduction, increased engine speed and start-stop. Many of these increase the stress on the bearing through higher loads, increased deformation, increased temperature and reduced oil film thickness. They also highlight an increased need to understand and predict the bearing behavior in order to design an optimized lubrication system.

Elastohydrodynamic (EHD) bearing analysis is a useful tool for addressing these issues. In an EHD simulation the Reynolds hydrodynamic lubrication equation for the oil film is coupled with the elastic deformations of the bearing in an iterative process in order to obtain converged solutions for the oil film pressure and oil film thickness. Mahle Engine Systems has developed and maintains an internal software code called SABRE-EHL for EHD bearing simulation. The code utilizes a finite difference scheme and includes oil film history and thermal energy models enabling predictions for oil film pressure, oil film thickness, power loss, oil flow and distributed temperature to be obtained (Wang 1999).

Abaqus is an integral part of the SABRE-EHL analysis process, providing data related to the structural stiffness of the housing, assembly deformations, inertia effects and journal/crankpin misalignment. This paper provides an overview of the different types of analysis that have been developed and deployed in order to extract the required input data for SABRE-EHL.

The target bearings are primarily the crankshaft bearings plus the small end bush (Figure 2), but can also include camshaft, balance shaft, oil pump and gear bearings/bushes.

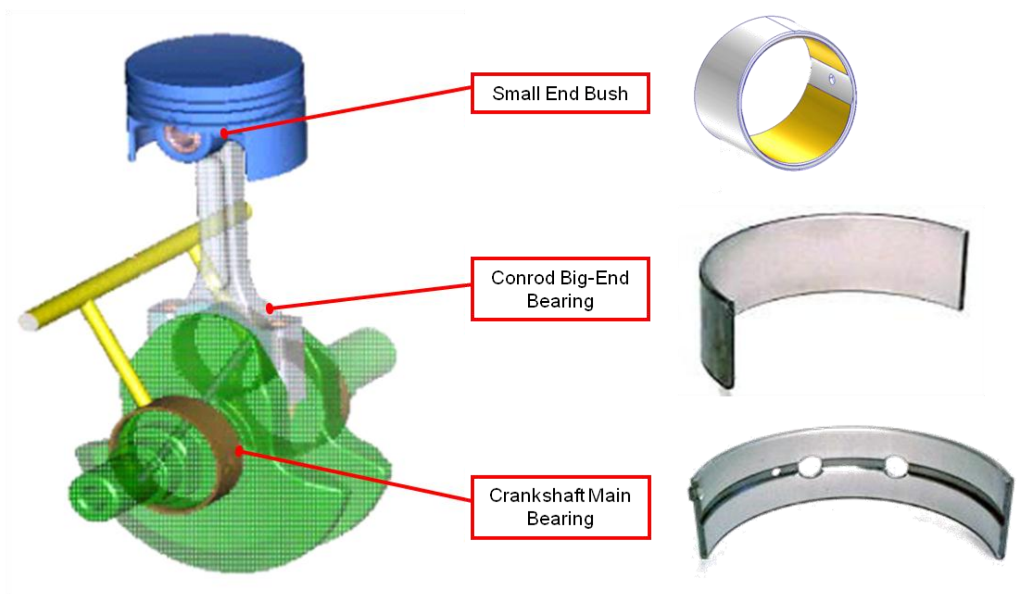

Figure 2: Engine crankshaft bearings.

2. Abaqus simulation for generating SABRE-EHL input

The simulation work flow for a connecting rod big-end bearing analysis is given in Figure 3. The baseline finite element analysis (FEA) models are currently created in a third party FEA preprocessor. There are four Abaqus/Standard simulation cases (indicated in the dashed-line box) used to generate input for SABRE-EHL - a stiffness matrix analysis (x2), a bearing fit analysis and a rod acceleration analysis. Extracted results are stored in a text file. In addition a fifth Abaqus/Standard simulation is possible, where bearing pressures from SABRE-EHL are applied back onto the FEA model (cycle pressure analysis). For a main bearing simulation, the procedure is very similar except a full crankshaft analysis is performed instead of a rod acceleration analysis.

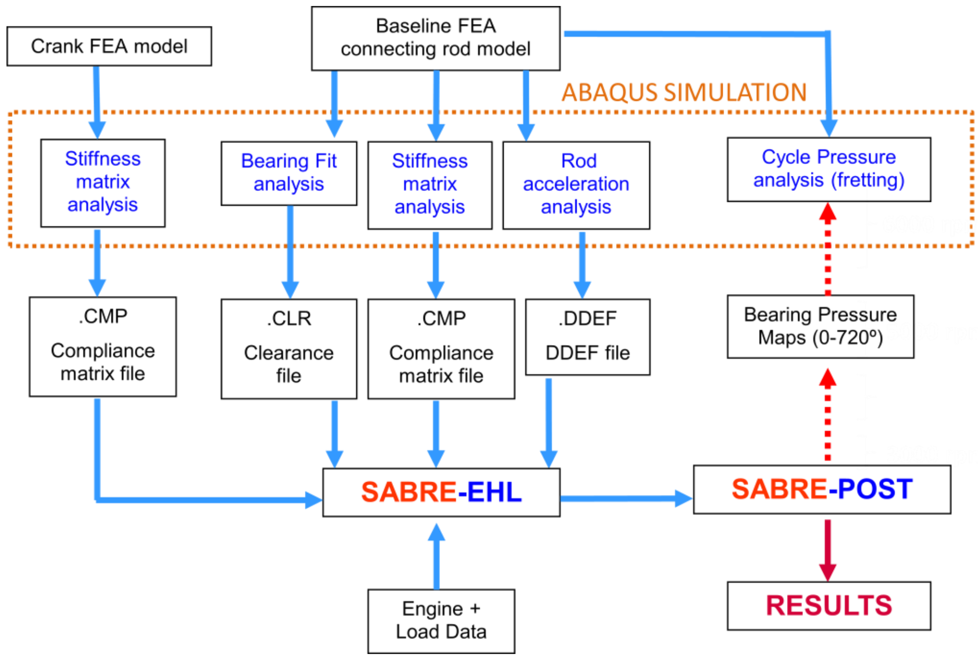

Figure 3: Simulation workflow for a SABRE-EHL analysis.

2.1 Stiffness matrix analysis

During the engine crankshaft cycle (0 - 720º for a 4 stroke engine) the connecting rod is pressed against the rotating crankshaft pin by the cylinder pressure and inertia loads. The resulting hydrodynamic pressure causes a deformation of the bearing shape, dependent on the magnitude of the load and the stiffness of the surrounding rod/crank structure. This effect is captured and included in SABRE-EHL via a stiffness matrix (Mian, 2002).

Typical FEA models for the connecting rod and crankshaft are shown in Figure 4. The main body of the model is meshed with tetrahedral elements (C3D10M). However, hexadedral elements are used for the bearing and crank pin, due to a requirement that the FEA model nodes match the rectagular finite difference lubrication grid used in SABRE-EHL. Tied contact is used to connect the two different element types.

A linear substructure step is defined requesting radial stiffness output for the bearing face nodes (*SUBSTRUCTURE GENERATE and *SUBSTRUCTURE MATRIX OUTPUT). The resulting analysis yields a stiffness matrix file (.mtx). A Fortran program is then used to invert the stiffness matrix to obtain a compliance matrix (.cmp). This program also applies a unit pressure to the compliance matrix generating a deformation plot. This is used as a visual check that the resulting compliance matrix is giving reasonable deformations.

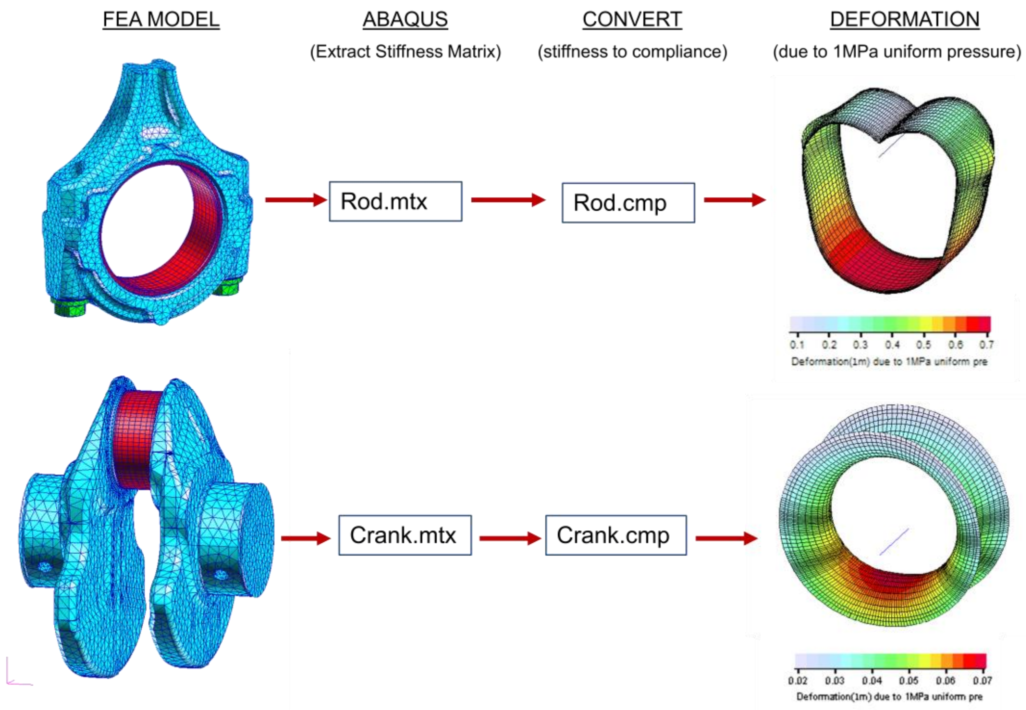

Figure 4: FEA models and resulting deformation.

2.2 Bearing fit analysis

In the bearing assembly process, the rod cap is bolted onto the main rod body - the bearing shells being clamped in place by an interference fit. Prior to this final assembly, the rod bore is machined circular when in the bolted-up state without bearing shells. The 'spring-back' out-of-round deformation which occurs on un-bolting needs to be included at the start of the bearing fit analysis.

The baseline FEA model used to extract the stiffness matrix is also used to perform the bearing fit analysis. Small sliding contact is defined between the bearing shells and rod bore. The initial design interference and the machining deformations are both included at the start of the analysis using a *CLEARANCE definition for all rod bore nodes in contact with the bearing back. A static, non-linear analysis is defined - Step 1: shrink-fit, Step 2: apply bolt load.

Nodal coordinates and deformations for the bearing face nodes are extracted and written to a text file. An external program reads this file and using a defined journal diameter calculates a radial clearance value for each node on the bearing face. Bearing profile design features such as eccentricity and joint face relief can be added to the clearance at this point. The results are stored in a bearing clearance file (.clr). This defines the initial static deformed bore shape used in SABRE-EHL. A typical deformed plot is shown in Figure 5, together with a comparison between a measured and predicted bearing bore shape.

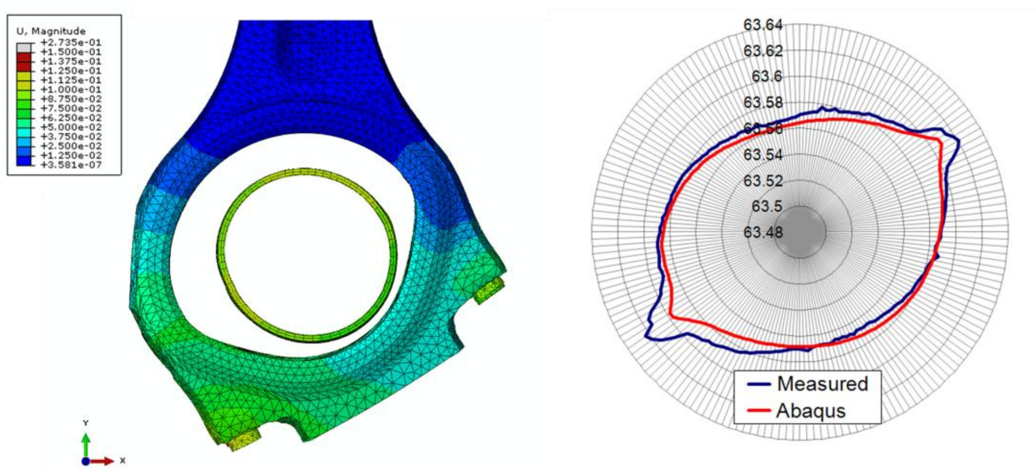

Figure 5: Bearing fit deformation and resulting clearance profile.

2.3 Connecting rod acceleration analysis

In addition to the stiffness deformations due to the reaction of the crankpin, the motion of the connecting rod generates inertia forces which cause deformations due to its own distributed mass (Merritt 2007).

An Abaqus/Standard analysis of the constrained connecting rod without a crank pin is used to obtain the bearing bore deformations due to the inertia of the distributed rod mass. A slider-crank mechanism gives rise to three primary acceleration components for the rod, linear acceleration (a) along the cylinder axis, rotational velocity (ω) and rotational acceleration (α) about the small end (Figure 6). The rod is constrained on a node at the centre of the small end (allowing rotation) and also in ‘X’ at a plane on the shank to prevent excessive bending under the side loads. *DLOAD Accelerations are applied to the rod in a series of linear static steps at 10º intervals through a single 0-360º crank cycle.

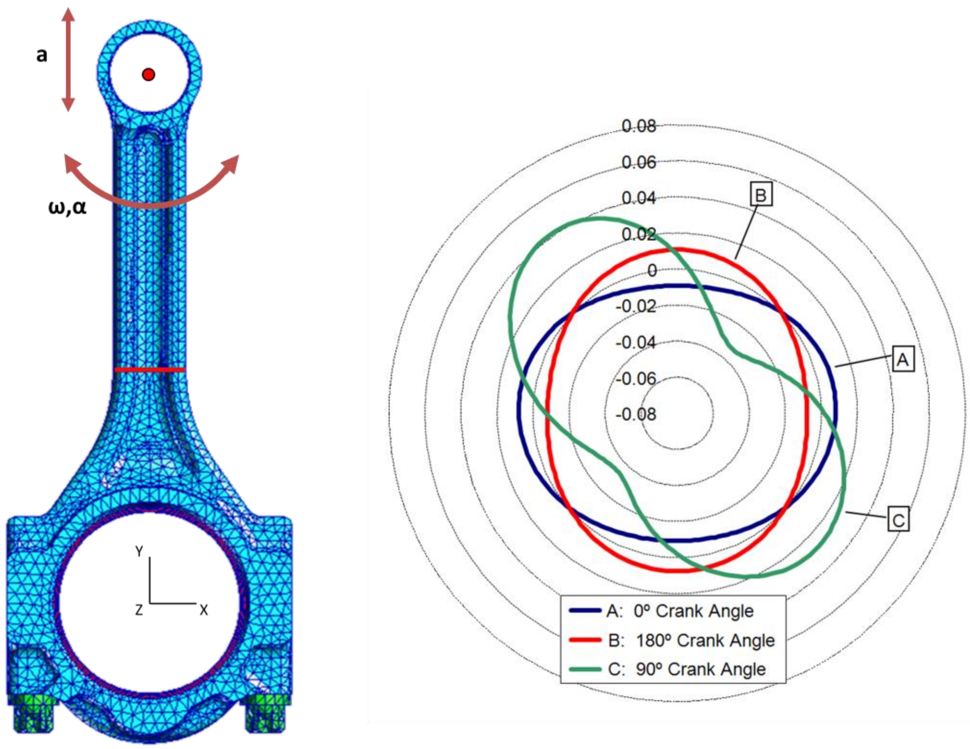

Figure 6: Applied accelerations and resulting bore deformation.

Nodal coordinates and deformations for the bearing face nodes are extracted and written to a text file. An external program reads this file, calculates the radial deformation and stores the results in a dynamic deformation file (.ddef). The resulting file contains bearing face node deformations at 2º intervals through the crank cycle (0-720°). During the SABRE-EHL analysis these deformations are combined with the initial static clearance and stiffness deformations to give the true bearing bore shape and operating clearance.

The bearing bore deformations for different positions in the crank cycle are shown in Figure 6 (6500 rpm load case). Significant deviations of up to 40μm are seen which is the same order of magnitude as the original static bearing clearance. The effect is speed dependant and will be less significant at low engine speeds.

2.4 Crankshaft cycle analysis

For a main bearing SABRE-EHL analysis, crankshaft bending has a significant influence on bearing performance. The bending effects how the loads are distributed to the main bearings and also causes misalignment between the main journal pins and bearings, leading to edge loading issues.

The solution to main bearing loading is statically indeterminate due to these bending effects and also due to non-linear effects in the oil film and clearance space. Therefore, a full non-linear Abaqus/Standard anaysis of the crankshaft is required. Results are extracted for main bearing loads and also the misalignment of the main journal pins.

The surface of each journal is connected to a reference node at its centre via a couple constraint. Connecting rod loads are applied to the rod pin reference nodes and centrifugal inertia is applied to the whole model. The effects of the clearance space and engine block stiffness are approximated using non-linear springs connecting a fixed block reference node to the the main journal pin reference node for each main bearing (Figure 7).

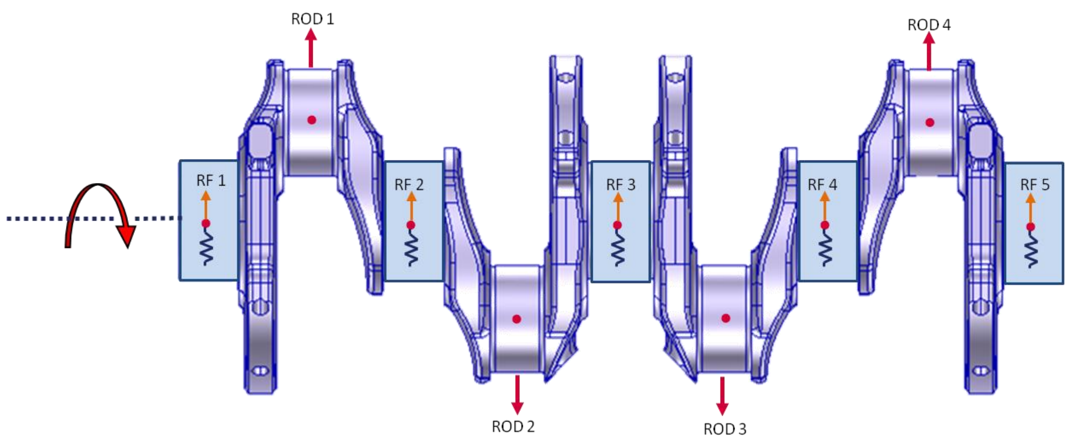

Figure 7: Crankshaft model set-up.

Forces are applied to the model in a series of non-linear static steps at 4º intervals through the complete crank cycle (0-720º). An example of crankshaft deformation under the peak cylinder firing load is shown in Figure 8. From the results, the journal pin misalignment is calculated for each crank interval through the cycle. Coordinates and deformations for the journal face nodes are extracted and written to a text file. An external program reads this file, calculates the radial misalignment, rotates the data relative to the 'fixed' main bearing reference frame and stores the results in a dynamic deformation file (.ddef). During the SABRE-EHL analysis these deformations are combined with the initial static clearance and stiffness deformations to give the true bearing bore shape and operating clearance.

The reaction forces at the engine block reference nodes are output to a text file. An external program reads this file, calculates the load and outputs a SABRE-EHL load file for each main bearing (Figure 9).

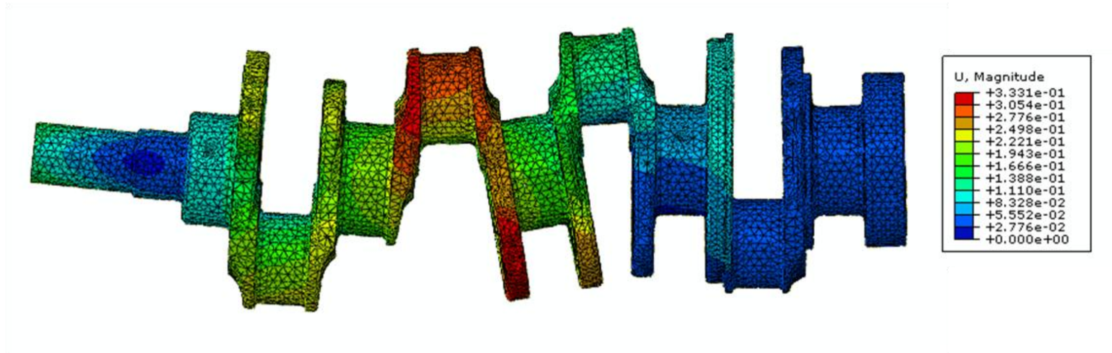

Figure 8: Crankshaft deformation due to cylinder no.2 firing @ 2200 rpm.

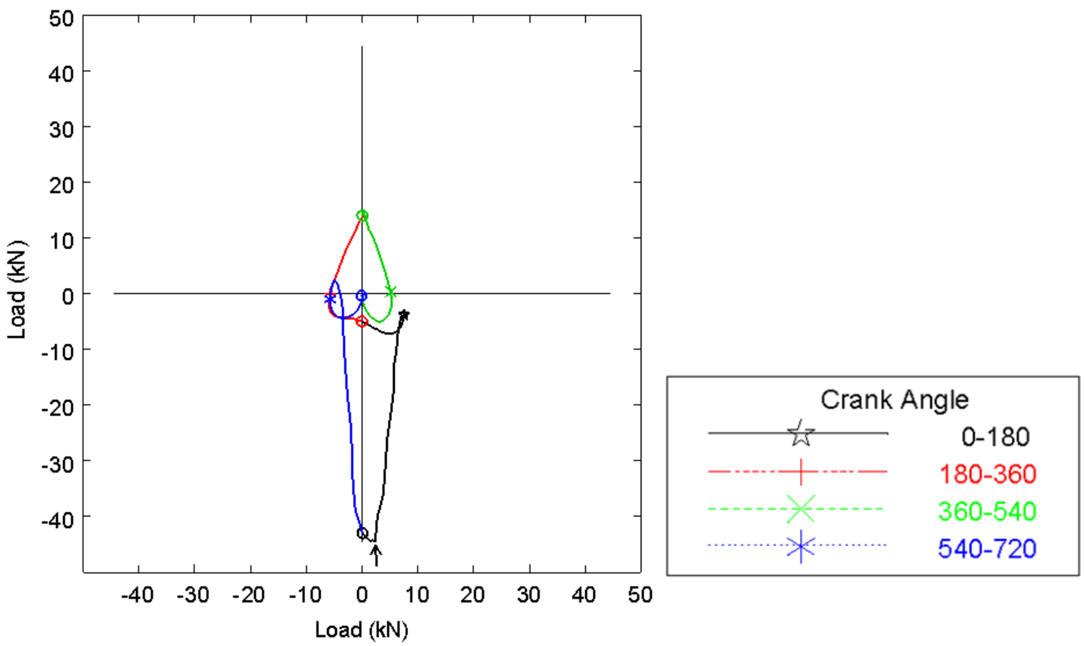

Figure 9: Load for main bearing no.1 - extracted from Abaqus FEA.

3. Engine test validation

A connecting rod instrumented with strain gauges has been tested in a 2.0L 4-cylinder gasoline engine. An aluminium linkage carrier is used to carry wires from the gauges to the engine block and then out to the recording instruments, enabling real time strain measurements to be taken. The instrumented rod together with the strain gauge locations is shown in Figure 10.

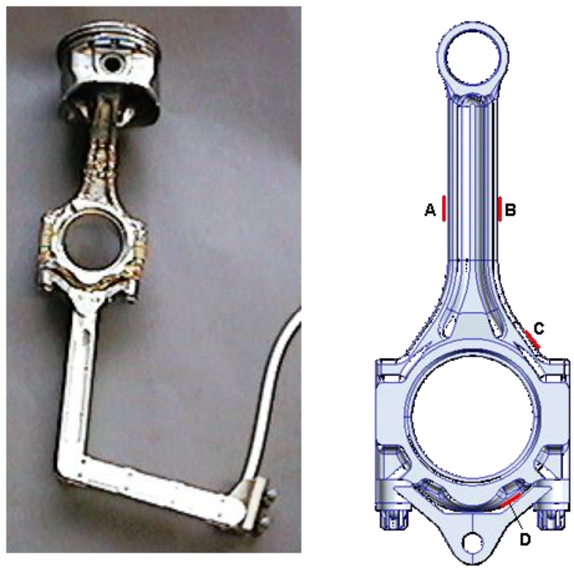

Figure 10: Instrumented connecting rod and strain gauge locations

An equivalent FEA model was constructed, including the connecting rod and linkage carrier and a SABRE-EHL analysis of the big-end bearing carried out. Bearing pressures were extracted and applied back onto the FEA model (cycle pressure analysis in Figure 3). In addition to the bearing pressues, the rod accelerations were also applied to the rod, giving the complete force balance that the rod would see in the engine. The Abaqus/Standard analysis is set up as a series of linear static steps at 10º intervals through the complete crank cycle (0-720º).

The comparison between measured and predicted strain is shown in Figure 11. The top graph shows good agreement for the rod shank axial strain. The middle graph (shank whipping strain) and the bottom graph (cap big-end eye strain) both show a good prediction of the general trends. An exact match is not expected since the Abaqus simulation does not include the linkage rods. The oscillations seen in the measured whipping strain are thought to be due to the 1st bending mode vibrations of the connecting rod at around 1625Hz. However, the influence of these vibrations is not seen in the measured big-end eye strains.

The overall good correlation gives confirmation that the correct bearing bore shape is being predicted and provides a validation of the FEA Abaqus method.

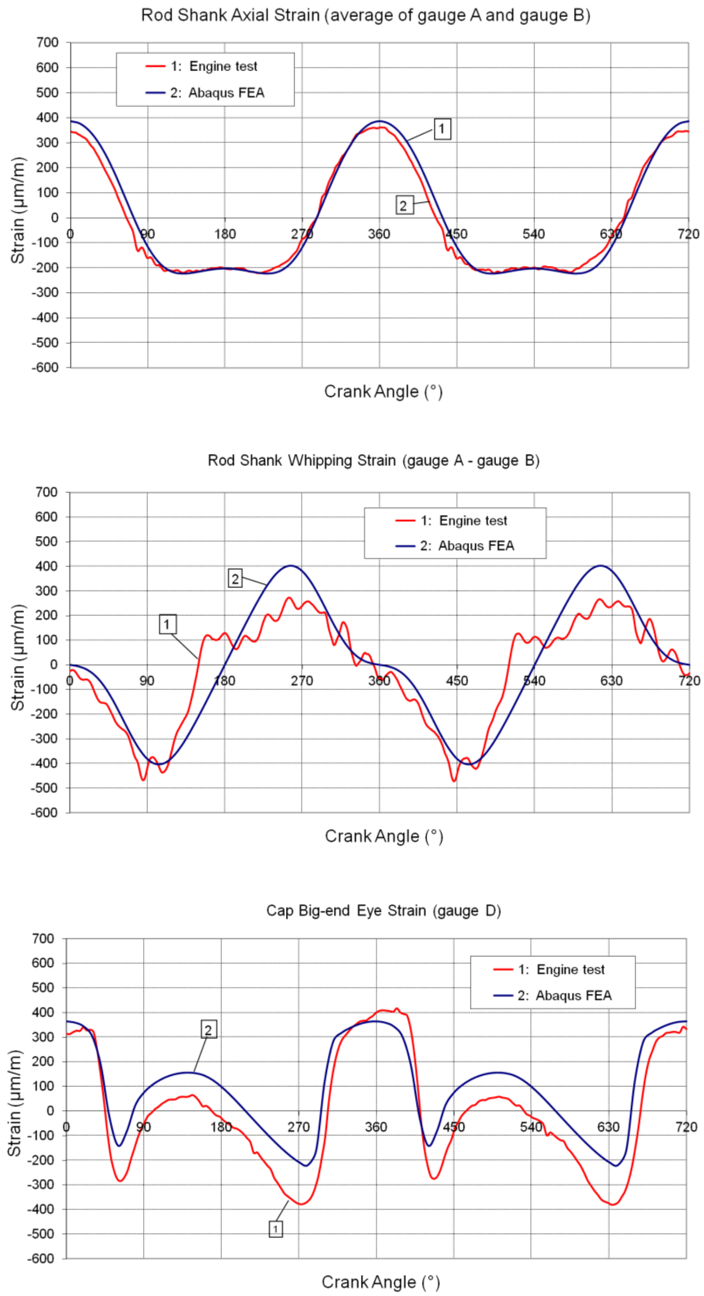

Figure 11: Rod shank strain, whipping strain and cap big-end eye strain.

4. SABRE-EHL results

This section gives some brief examples of SABRE-EHL results and also demonstrates how the Abaqus generated input data related to stiffness, bearing fit and dynamic deformation influences the pressure generation and oil film thickness in the bearing.

Figure 12 shows the 3-D oil film pressure map at TDC firing for a connecting rod bearing. Results are shown for two rod designs, one open shank and one closed shank, showing how the stiffness distribution of the material surrounding the bearing significantly influences the pressure generation in the oil film.

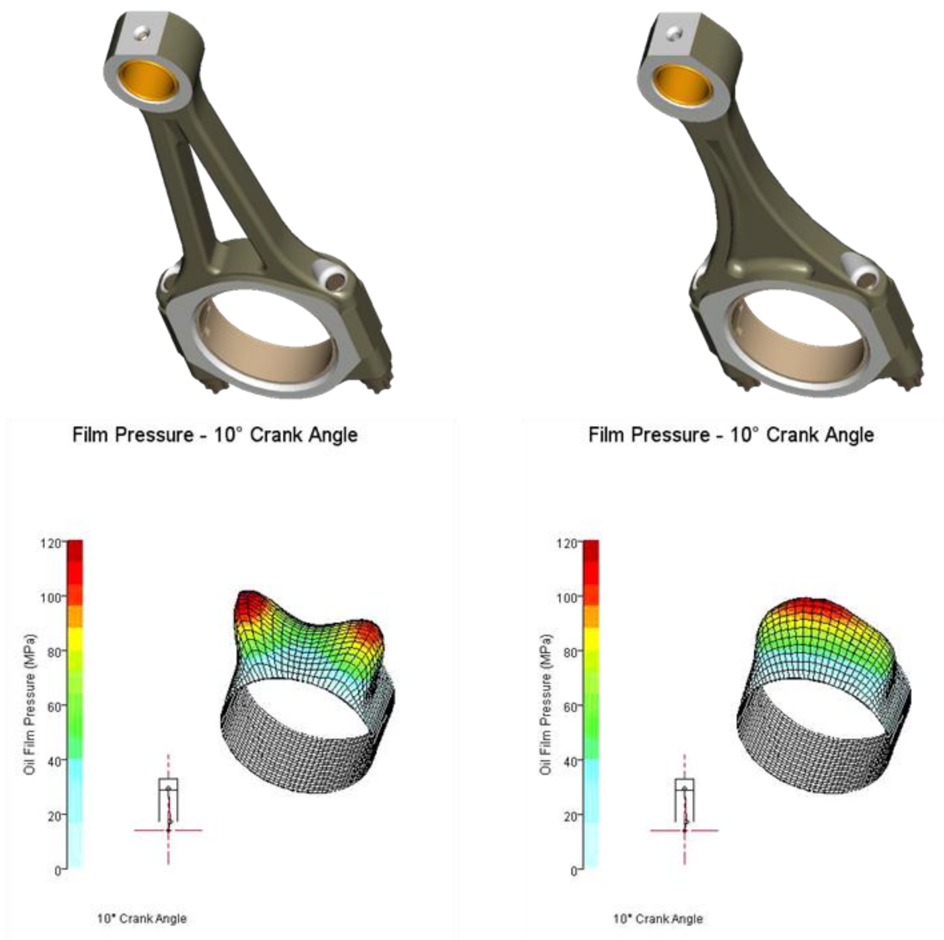

Figure 12: SABRE-EHL 3-D oil film pressure map for two rod designs.

For a main bearing SABRE-EHL analysis, the thermal expansion of the engine block can significantly influence the bearing bore shape. These effects can be included by adding a temperature step at the end of the bearing fit simulation. The polar plot (Figure 11) shows how thermal expansions can significantly distort the bearing clearance shape (@140ºC engine operating temperature). The resulting 2-D oil film pressure map (Figure 13) shows how a pressure 'spike' can be concentrated at the point of minimum clearance, potentially leading to bearing fatigue.

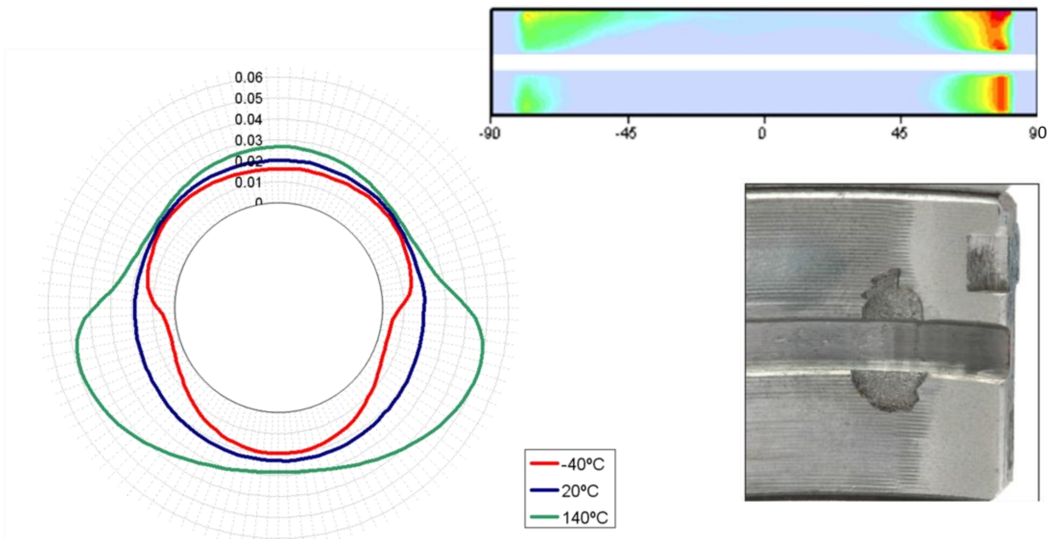

Figure 13: Effect of temperature on bearing bore shape. Resulting oil film pressure map and related bearing lining fatigue damage.

The cycle pressure analysis used in the engine test validation, as well as providing stresses and strains within the housing and bearing structures, can also be used to investigate contact interactions between the bearing back and inner housing bore. Micro-slip between the two surfaces can cause problems such as bearing rotation, surface fretting damage and in extreme cases cracks and failure in the housing due to fretting induced fatigue.

Contact interaction parameters from the Abaqus analysis can be used to derive a fretting parameter (circumferential slip * circumferential shear stress) and also a 'Ruiz' parameter. ‘Ruiz’ combines fretting potential with tensile stress on the inner housing bore giving an indication of fretting induced fatigue fracture (circumferential slip * circumferential shear stress* hoop stress). Figure 14 shows the 'Ruiz' parameter plotted on the inner rod bore showing good correlation with the fracture location for a tested connecting rod (Merritt 2004).

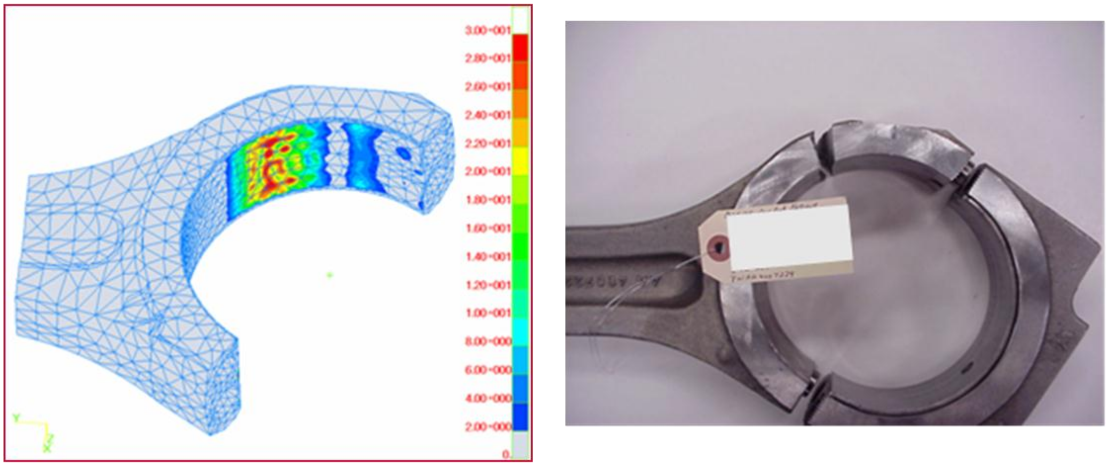

Figure 14: Abaqus FEA 'Ruiz' parameter compared with test fracture.

Figure 15 shows the results for a SABRE-EHL camshaft bush analysis. The 2-D oil film thickness intensity map is compared with the bush wear marks from an engine test. This is a demonstration of how shaft bending, in this case due to a power take-off load on the end of the camshaft, can cause edge loading and a bias in the contact pattern. This effect is included in SABRE-EHL using dynamic deformations from the Abaqus camshaft loading simulation.

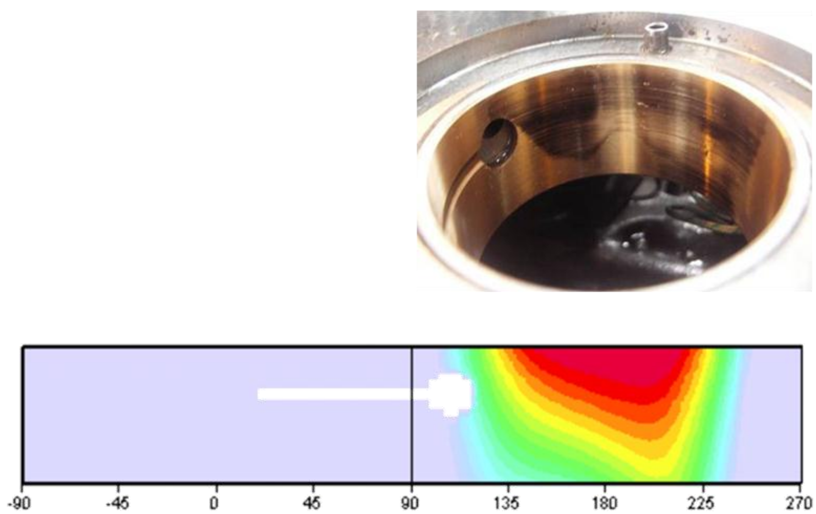

Figure 15: Camshaft bush oil film thickness intensity - compared with test bush.

5. Conclusions

This paper has demonstrated a number of Abaqus/Standard simulations which can be deployed to pre-process the parameters influencing the bearing clearance shape during an engine cycle simulation. These include the stiffness of the housing and crank pin, the bearing fit assembly deformations, connecting rod distributed mass inertia deformations and misalignments due to shaft bending. These effects can be pre-processed in Abaqus and then combined in the SABRE-EHL code to give a true bearing bore shape and clearance profile at each crank angle. This is critical for accurately predicting the important bearing performance parameters - such as the oil film pressure, oil film thickness, power loss and oil flow.

Good correlation between measured and predicted connecting rod strain, along with good comparison of SABRE-EHL results with damaged engine test bearings, confirm the effectiveness of this method.

6. References

1. Mian,O., Merritt, D and Wang, D, "The effect of crankshaft flexibility on EHL of connecting rod bearings", SAE 2002-01-0295.
2. Merritt, D and Guangrui, Z, "The prediction of connecting rod fretting and fretting induced fatigue fracture", SAE 2004-01-3015
3. Merritt, D , Mian, O and Wang, D, "Connecting rod EHD analysis including inertia effects due to the distributed rod mass", SAE 2007-24-0134.
4. Wang D., 1999, “Development and Validation of Finite Difference SABRE-EHL Code,” GVRR Technical report, No. 1046, Mahle Engine Systems, Rugby, UK

7. Acknowledgements

The author would like to thank colleagues in the scientific services department at Mahle Engine Systems who have contributed to the development of the SABRE code and related Abaqus FEA procedures. Also, the testing department who performed some of the measurements presented in the paper.